Revista de Chimie
https://revistadechimie.ro
https://doi.org/10.37358/Rev.Chim.1949

Potency of Three Brown Seaweeds Species as the Inhibitor of RNA-dependent RNA Polymerase of SARS-CoV-2

MUHAMAD FIRDAUS*, RAHMI NURDIANI, INDRI NOVITA ARTASASTA, SAYYIDAH MUTOHAROH, ONI PRATIWI
Brawijaya University, Faculty of Fisheries and Marine Sciences, Department of Fisheries Product Technology, Jalan Veteran, Malang – 65145, Indonesia

Abstract: *The objective of this study was to evaluate the binding activity of bioactive compounds from three brown seaweed on RNA-dependent RNA polymerase (RdRp) of SARS-CoV-2 by docking method. The bioactive identification of Sargassum cristaefolium, S. echinocarpum, and Padina australis was carried out using HPLC-HRMS. The ligand structures in PDB format were obtained from the PubChem website and the RdRp from the RCSB website. The binding affinity of the interaction of bioactive components with the RdRp Covid-19 was determined by docking method using AutoDock Vina on PyRx software. The visualization of 2D and 3D interactions between ligands and macromolecules were carried out with the Biovia Discovery Studio and PyMol software. The decoction of S. cristaefolium, S. echinocarpum, and P. australis contained ninety one compounds, and there were twenty compounds with a strong affinity for RdRp. Rhamnetin was a compound of the Sargassum species have the strongest binding affinity of -7.6 kcal/mol. Its affinity bonds were hydrogen bonds in Val315, Arg349, Phe396, Asn628, and hydrophobic bonds in the form of bonds to π-ε and π-alkyl from Pro461. Taribavirin bound to RdRp in hydrogen bonds at Thr393, Thr394, and Phe396 and bound hydrophobically to π-alkyl from Cys395. Rhamnetin has the same binding affinity region as taribavirin, which was the subdomain finger of the RdRp. In conclusion, rhamnetin is a compound of Sargassum sp that can inhibit the replication and transcription of RdRp SARS-CoV-2 and further studies using the molecular dynamics method on the mechanism of interaction between rhamnetin and the viral RdRp of SARS-CoV-2 are mandatory.*

Keywords: *Brown algae, Decoction, HPLC HRMS, in silico, RdRp*

1. Introduction

Covid-19 is an acute respiratory disease which was first discovered in Wuhan, China and has now spread throughout the world [1]. This disease suffered by a person infected with the Covid-19 virus. This virus classified as a new genus of beta coronavirus. It appears in severe acute respiratory syndrome coronavirus (SARS-CoV-2) and some bat coronaviruses. Coronavirus has an RdRp that functions for virus replication and transcription. RdRp has three domains, namely the thumb, palm and finger subdomains, these subdomains playing a role in the entry of nucleotide triphosphate, binding templates and polymerization, as well as other functions still related to the three previous functions. The active site of this enzyme being on the finger subdomain. The finger subdomain plays a vital role as the active site of the template for RNA binding and polymerization. This subdomain has catalytic residues at residues 366-581 and 621-679 [2, 3]. This enzyme plays a role in the synthesis of RNA and the replication and transcription cycle of viruses. Inhibiting the activity of these enzymes can be the principal role of inhibiting this virus [2, 3]. Taribavirin is a synthetic nucleoside analogue of ribofuranose that inhibits the viral RNA synthesis of the influenza virus by attaching itself to the nucleic acid of this virus. The use of this antiviral agent can result in anaemia, diarrhoea, fatigue, and drowsiness, and if consumed chronically, it can induce hepatitis C [4]. Meanwhile, natural ingredients are known to have less frequent side effects with more complex therapeutic effects [5].

Brown seaweed is one of the many biotas that grow and spread in tropical and subtropical waters.

email: muhamadfir@ub.ac.id

Sargassum is a species of brown seaweed which contains a lot of natural ingredients and has been used for more than 1500 years as Traditional Chinese Medicine for the treatment of several diseases [6-11]. Brown seaweed species have studied for its ability as an antivirus, namely avian viruses, cytomegalic and measles viruses and herpes simplex viruses of types 1 and 2 [12]. The polysaccharides derivatives of brown algae can inhibit the replication of these viruses. However, its ability to inhibit the Covid-19 viruses, especially as an inhibitor of RdRp activity, is currently unknown; besides, the technology of separating polysaccharides derivatives from seaweed is still quite complex [13]. Many studies have shown that bioactive from natural ingredients obtained by decoction. The use of Chinese herbal decoction can specifically reduce the severity of people with Covid-19. The decoction is known as an easy and cheap natural extraction technique because it is only enough to boil the materials in water [14]. The purpose of this study was to evaluate the decoction of bioactive compounds from *S. cristaefolium*, *S. echinocarpum*, and *P. australis* as inhibitors of the RdRp activity using the in-silico method.

2. Materials and methods

2.1. Materials

Brown seaweed tested were *S. cristaefolium*, *S. echinocarpum*, and *P. australis*. The solvents used were aquadest, acetonitrile, and formic acid (HPLC grade). The material used in the docking analysis was the structure of the test ligand in the form of a compound identified from brown algae downloaded from the Pubmed database in SDF format.

The tool used to identify brown seaweed active compounds was the HPLC HRMS Thermo Scientific Dionex Ultimate 3000 RSLC Nano using a Hypersil GOLD aQ column (50 x 1 mm x 1.9 u particle size). The hardware used for the in-silico method was a laptop (HP Intel® Core ^{TM}i3-5005U) with a Microsoft Windows 10 operating system. The software packages used for the docking analysis were Open Babel GUI version 2.4.1 [15], PyMOL 1.7.4 Edu (Schrödinger) [16], Biovia Discovery Studio 2019 (Dassault Systèmes Biovia Corp.) [17], and PyRx 0.8 (The Scripps Research Institute) [18].

2.2. Methods

Brown seaweeds were obtained from Talango Island waters, Sumenep district, East Java Province, Indonesia. The samples washed thoroughly with clean seawater and transported immediately using separate cold boxes for each species to the Faculty of Fisheries and Marine Sciences at Brawijaya University in Malang. East Java. The samples were washed with running water to remove dirt. Seaweed samples were then cut into smaller pieces before they were decocted in water (1: 6.7: w / v) for 23 min at a temperature of 90°C. Afterwards, the extract was cooled to room temperature and then filtered with Whatman No. 40 paper to obtain the filtrate. The filtrate was then diluted with water containing 0.1% formic acid and vortexed for 1 min. Afterwards, the supernatant was filtered by a 0.22 μm of syringe filter and placed in a vial. The vials were placed in the autosampler and then injected into the HPLC-HRMS (Thermo ScientificTM).

The column temperature was 30°C and the solvent system consisted of solvent A (water with 0.1% formic acid) and solvent B (acetonitrile with 0.1% formic acid). The mobile phase flow rate of 40 μm L/min was run in a gradient ratio of solvents A and B (95: 5 at min 0-15, 40:60 at min 15-22 and 5:95 ratio at 22-25 min). The detected chromatogram identified based on the identity of the compounds contained in the Compound Discoverer, mzCloud MS / MS Library.

The 3D ligand structures of the brown algae compounds and taribavirin were obtained from the website https://pubchem.ncbi.nlm.nih.gov/ in the form of SDF format and then changed to PDB using Open Babel. Taribavirin used as a control was the inhibitor of RdRp of the influenza virus [4]. Before the docking process, taribavirin and the identified compounds of brown algae were first optimized with the OpenBabel. These ligands then minimized its energy to optimize its conformation. The results of the minimization were then formatted in pdbqt and were then ready for the docking process. The macromolecule was RdRp from the SARS-CoV-2 (ID: 6m71), which was downloaded in PDB format.

The RdRp PDB format of the SARS-CoV-2 (ID: 6m71) was obtained from http://www.rcsb.org/ [2]. RdRp as macromolecule in *.pdb format was converted into *.pdbqt format using the PyRx. Each ligand was in a flexible state that interacts with macromolecule under rigid conditions. AutoDock Vina was used to simulating the docking of test ligands and comparison ligand against RdRp [18]. All calculations were executed via a grid-box size of x = 74.81 Å, y = 84.54 Å, z = 85.72 Å, with a grid center of x = 120.05 Å, y = 123.86 Å, z = 120.15 Å. An exhaustiveness search parameter of 8 was used to predict the binding affinities due to the probability of finding the global minimum of the scoring functions. The docking results were evaluated, and the best value (ΔG was the most negative) was observed in the area of the ligands attached to the macromolecule. Interactions in the form of hydrogen bonds, hydrophobic bonds, and electrostatic bonds and bond distances were visualized in 2D and 3D with the Discovery Studio and PyMOL with an interaction radius of 5 Å [16, 17].

3. Results and discussions

3.1. Identity of chemical compounds of *S. cristaefolium, S. echinocarpum,* and *P. australis*

The brown seaweed samples *S. cristaefolium, S. echinocarpum,* and *P. australis* contained ninety one compounds in which consisted of sixty one, fifty, and sixty one bioactive compounds, respectively (Table 1). *Sargassum* sp and *P. australis* are among brown seaweed species that are widespread in tropical and subtropical waters. These biotas contain many phytochemicals, including phenols, alkaloids, tannins, steroids, glycosides, saponins, and flavonoids [6, 7].

Tabel 1. Chemical compounds of three brown seaweeds and their binding affinity

No	Compounds	*Sargassum cristaefolium*	*Sargassum echinocarpum*	*Padina australis*	Binding Affinity (kcal/mol)
1	D-(-)-Glutamine	√	√		-4.7
2	Betaine	√	√	√	-3.8
3	L(-)-Carnitine			√	-4.3
4	DL-Glutamine			√	-5
5	DL-Stachydrine			√	-4.5
6	DL-Carnitine	√	√		-4.5
7	N-Acetylputrescine		√		-4.5
8	L-Glutamic acid	√	√	√	-4.8
9	N-Methyl-D-aspartic acid (NMDA)	√			-5.1
10	Acetylcholine	√			-5.2
11	Hymexazol	√			-4.2
12	Uracil	√		√	-5.1
13	Adenosine 3'5'-cyclic monophosphate			√	-7.3
14	2-Aminophenol			√	-4.5
15	Valine	√		√	-4.3
16	L-Pyroglutamic acid	√	√	√	-5.1
17	Adenine	√	√	√	-5.6
18	Uric acid		√		-6.5
19	N6-Acetyl-L-lysine	√	√	√	-4.9
20	6-Aminocaproic acid		√		-4.6
21	DL-Tryptophan		√		-6.1
22	L-Histidinol		√		-4.8
23	4-Guanidinobutyric acid	√		√	-4.7
24	Nicotinic acid	√		√	-5.1
25	Isocytosine	√		√	-4.9
26	Acetyl-β-methylcholine	√		√	-3.8
27	Nicotinamide	√	√		-4.7
28	Hypoxanthine	√		√	-5.3
29	Guanine	√	√	√	-6.3

30	2-Aminonicotinic acid	√	√		-5.2
31	Obscurolide A1	√	√	√	-6.7
32	Desthiobiotin		√		-4.9
33	4-Hydroxybenzaldehyde		√		-4.5
34	3,4-Dihydroxyphenylpropionic acid	√			-5.7
35	Adenosine	√	√	√	-6.7
36	Inosine			√	-6.4
37	2-Hydroxycinnamic acid		√	√	-5.5
38	Valylproline	√			-6.8
39	2'-Deoxyadenosine	√		√	-6.1
40	L-Norleucine	√	√	√	-4.5
41	Acetophenone	√	√	√	-5.7
42	Isonicotinic acid 1-oxide	√	√		-4.8
43	Propionylcarnitine		√		-4.5
44	Pyrogallol	√	√	√	-5.2
45	Thymine			√	-5.3
46	Vasicinone	√			-6.4
47	Pirbuterol	√			-6
48	Rhamnetin	√	√		-7.6
49	4-Piperidone		√		-3.6
50	3,4-Dihydroxybenzaldehyde	√			-5.3
51	L-Phenylalanine	√		√	-5.2
52	Panthenol			√	-4.8
53	Isoamylamine	√			-3.8
54	δ-Valerolactam	√		√	-4.2
55	N-Butylbenzenesulfonamide	√	√	√	-5.3
56	trans-3-Indoleacrylic acid	√	√	√	-6
57	4-Indolecarbaldehyde		√		-5.4
58	Caprolactam	√	√	√	-4.4
59	6-Methylquinoline			√	-5.8
60	1-Methylxanthine			√	-6.1
61	N3,N4-Dimethyl-L-arginine		√		-5.3
62	7-Methylxanthine	√	√		-6.1
63	Dibenzylamine	√	√	√	-6.1
64	2-Hydroxybenzothiazole	√	√	√	-5.2
65	Ageratriol	√		√	-6.3
66	19-Nortestosterone			√	-6.9
67	Cyclohexyl phenyl ketone	√		√	-6.4
68	DEET	√	√	√	-5.2
69	Nootkatone	√	√	√	-6.7
70	2,2,6,6-Tetramethyl-1-piperidinol (TEMPO)	√	√	√	-5
71	4-(Dimethylamino)benzophenone	√	√	√	-6.3
72	D-(+)-Camphor	√	√	√	-5.5
73	(3S)-3-Methyl-5-[(1S,8aR)-2,5,5,8a-tetramethyl-4-oxo-1,4,4a,5,6,7,8,8a-octahydro-1-naphthalenyl]pentanoic acid			√	-6.3
74	3-Methyl-5-[(1S,2R,4aR)-1,2,4a,5-tetramethyl-7-oxo-1,2,3,4,4a,7,8,8a-octahydro-1-naphthalenyl]pentanoic acid			√	-7
75	Decanamide		√		-4.8
76	Dimethyl 2,6-naphthalenedicarboxylate	√			-7.1
77	N1-Hydrazino[3-(methylthio)anilino] methylidenebenzene-1-sulfonamide	√	√	√	-7.1
78	1-Tetradecylamine	√	√	√	-4.4

79	α-Pyrrolidinopropiophenone		√	√	-5.7
80	3,5-di-tert-Butyl-4-hydroxybenzaldehyde	√	√	√	-5.8
81	Tetranor-12(S)-HETE	√	√	√	-5.2
82	Zearalenone		√		-7.3
83	α-Eleostearic acid	√		√	-4.9
84	Dibutyl phthalate	√	√	√	-5.5
85	Cycluron		√	√	-5.5
86	n-Pentyl isopentyl phthalate	√	√	√	-6.3
87	N-Desmethylclomipramine			√	-6
88	4-tert-Butylcyclohexyl acetate	√		√	-5.2
89	4-Methoxycinnamic acid	√			-5.8
90	Triethanolamine	√		√	-4.4
91	Choline	√		√	-3.6
	taribavirin				-6.1

3.2. Molecular docking

There were twenty compounds that have a stronger affinity energy than taribavirin, e.g. adenosine-3'5'-cyclic monophosphate, uric acid, guanine, obscurolide A1, adenosine, inosine, valylproline, vasicinone, rhamnetin, ageratriol, 19-nortestosterone, cyclohexylphenyl ketone, nootkatone, 4-(di-methylamino) benzophenone, (3S) -3-methyl-5 - [(1S, 8aR) -2,5,5,8,8-tetramethyl-4-oxo-1,4 4a,5,6,7,8, 8a-octahydro-1-naphthalene] pentanoic acid, 3-methyl-5 - [(1S, 2R, 4aR) -1,2,4a, 5-tetramethyl-7-oxo-1,2,3,4,4a,7,8,8a-octahydro-1-naphthalene] pentanoic acid, dimethyl-2,6-naphthalenedicarboxylate, N1-hydrazino [3- (methylthio) anilino] methylidenebenzene-1-sulfonamide, zearalenone, and n- pentyl isopentyl phthalate, respectively (Table 1).

The docking results showed that rhamnetin had the strongest binding affinity for RdRp (-7.6 kcal/mol) (Table 1). Rhamnetin is a mono-metoxyflavone, which is a derivative of methylated quercetin. This compound has the potential to inhibit the protease activity of SARS-CoV-2 [19, 20]. Its bonds to RdRp included hydrogen bonds in Val315, Arg349, Phe396, Asn628, and hydrophobic bonds in Pro461 in the form of π-ε, and π-alkyl bonds. As a hydrogen donor, rhamnetin interacts with Val315 at a distance of 2.61828 Å and with Pro461 at a distance of 3.86226 Å. Arg349 bonded rhamnetin with a distance of 4.41304 Å, Phe396 with a distance of 4.23149 Å and Asn628 with a distance of 3.02164 Å (Figure 1). The hydrogen bonds between rhamnetin and the RdRp residue, namely Phe396 and Asn628, and the hydrophobic bonds of rhamnetin with the RdRp residue of Pro461 are located in the finger subdomain. These bindings indicate that rhamnetin binds on the active side of RdRp. Taribavirin binds RdRp residues via the hydrogen bonds on Thr393 and Cys395 by hydrophobic bonds; meanwhile, Phe396 and Thr394 of RdRp residues bind taribavirin only by hydrogen bonds (Figure 2). The hydrogen and hydrophobic binding between taribavirin and the RdRp residues in the finger subdomain and it indicate that taribavirin also binds to the active site residues of RdRp.

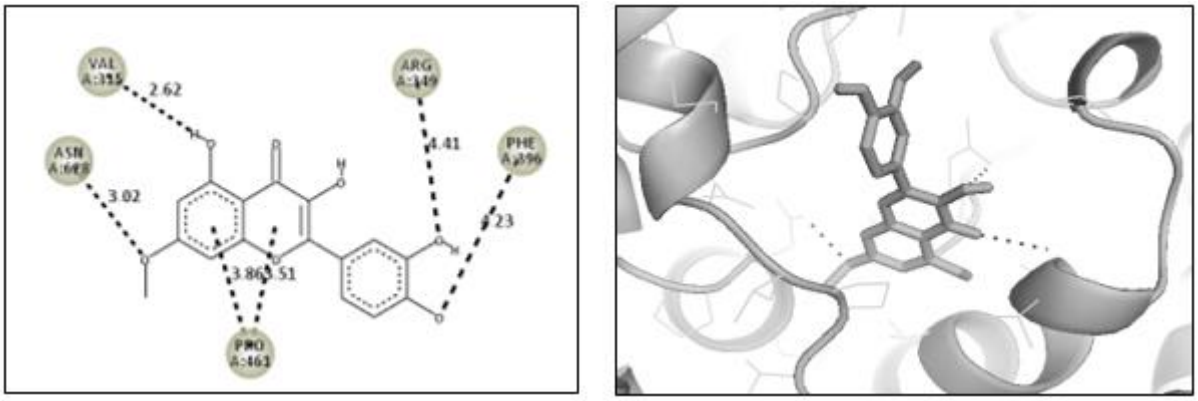

Figure 1. 2D and 3D interaction between rhamnetin and RdRp of covid-19 virus

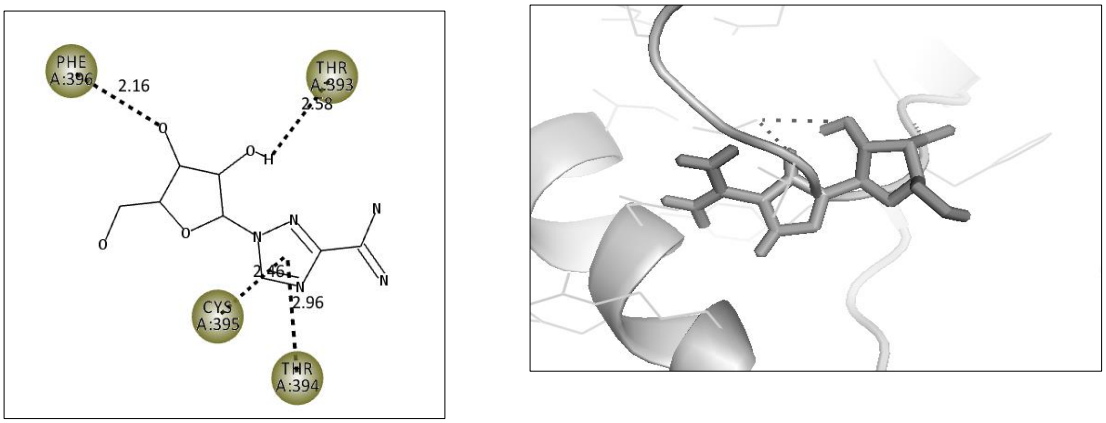

Figure 2. 2D and 3D interaction between taribavirin and RdRp of covid-19 virus

The molecular docking results showed that rhamnetin had lower binding energy of -7.6 kcal/mol compared to taribavirin of -6.6 kcal/mol (Table 1). The difference of the binding energies between rhamnetin and taribavirin is possible due to the different binding to the residue or the amino acid of RdRp. The properties of the residues involved in the interaction determine the stability of the ligand-receptor interaction [21]. Rhamnetin binds to four amino acid residues from the RdRp, namely Val315, Arg349, Phe396 and Asn628. These amino acids have high hydrophilic properties, and these amino acids interact with water molecules on the surface of the receptor. This interaction can maintain the stability of the interior of the structure of the RdRp compared to its hydrogen bonding with taribavirin, which occurs only in Phe396. The identical of rhamnetin and taribavirin binding to Phe396 means that Phe396 is one of the binding site residues of the RdRp.

4. Conclusions

Our docking results show a higher binding affinity for taribavirin within RdRp's active sites containing the following residues: Thr393, Phe396, Thr394, and Cys395. The lowest binding affinity among the natural compounds of *S. cristaefolium*, *S. echinocarpum*, and *S. aquifolium* was found for rhamnetin. Rhamnetin presented the most significant fitting score value of -7.6 kcal/mol for the active sites of the RdRp structure of SARS-CoV-2 virus. Further investigations using Molecular Dynamics methods on the interaction mechanisms between the ligands and viral RdRp of SARS-CoV-2 are mandatory.

Acknowledgments: This study funded by PNBP scheme of Faculty of Fisheries and Marine Sciences, Brawijaya University (No. 37/UN10.F06.06/2020).

References

1. EARAR, K., ARBUNE, M., DOROBAT, C.M., GURAU, G., ANTONIAC, I., INDREI, L.L., Emergency COVID-19: A surprising pandemic. *Rev. Chim*, **71**(3), 2020, 307-311.
2. GAO, Y., YAN, L., HUANG, Y., LIU, F., ZHAO, Y., CAO, L., et al., Structure of the RNA-dependent RNA polymerase from COVID-19 virus. *Science*, **368**, 2020, 779-782.
3.VENKATARAMAN, S., PRASAD, B.V.L.S., SELVARAJAN, R., RNA Dependent RNA Polymerases: Insights from Structure, Function and Evolution. *Viruses*, 2018, doi: 10.3390/v10020076.
4. FISCHER, W.A., HAYDEN, F., Antivirals for Influenza: Novel Agents and Approaches. In: Georgiev V.S., Western K.A., McGowan J.J. (eds) National Institute of Allergy and Infectious Diseases, NIH. Infectious Disease. Humana Press. 2008, https://doi.org/10.1007/978-1-59745-569-5_19

5.BESEDNOVA, N., ZAPOROZHETS, T., KUZNETSOVA, T., MAKARENKOVA, I., FEDYANINA, L., KRYZHANOVSKY, S., MALYARENKO, O., ERMAKOVA, S., Metabolites of Seaweeds as Potential Agents for the Prevention and Therapy of Influenza Infection. *Mar Drugs,* **17**, 2019, 373, doi:10.3390/md17060373.
6. MEHDINEZHAD, N., GHANNADI, A., YEGDANEH, A., Phytochemical and biological evaluation of some *Sargassum* species from Persian Gulf. *Res in Pharm Sci,* **11**(3), 2016, 243-249.
7.KANIMOZHI, A.S., JOHNSON, M., RENISHEYA, J.J.M.T., Phytochemical composition of *Sargassum polycystum* C. Agardh and *Sargassum duplicatum* J. Agardh. *Int J Pharm Pharm Sci,* **7**, 2015, 393-397.
8.YENDE, S.R., HARLE, U.N., CHAUGULE, B.B., Therapeutic potential and health benefits of *Sargassum* Species. *Pharmacog Rev,* 2014, doi: 10.4103/0973-7847.125514.
9.FIRDAUS, M., CHAMIDAH, A., *Sargassum polycystum* extract affects tumor necrocis factor alpha and interleukin-6 expression in streptozotocin–induced diabetic rats. *Asian J Pharm Clin Res,* **11,** 2018, 337-339.
10.SUN, Y., CHEN, X., ZHANG, L., LIUA, H., LIU, S., YU, H., et al., The antiviral property of *Sargassum fusiforme* polysaccharide for avian leukosis virus subgroup J in vitro and in vivo. *Int J Bio Macromol,* **138,** 2019, 70–78.
11.LIU, L., HEINRICH, M., MYERS, S., DWORJANYN, S.A., Towards a better understanding of medicinal uses of the brown seaweed Sargassum in Traditional Chinese Medicine: A phytochemical and pharmacological review. *J Ethnopharm,* **142**, 2012, 591-619.
12.PENG, Y., XIE, E., ZHENG, K., FREDIMOSES, M., YANG, X., ZHOU, X., et al., Nutritional and Chemical Composition and Antiviral Activity of Cultivated Seaweed *Sargassum naozhouense* Tseng et Lu. *Mar Drugs,* 2013. doi: 10.3390/md11010020.
13.SHI, Q., WANG, A., LU, Z., QIN, C., HU, J., YIN, J., Overview on the antiviral activities and mechanisms of marine polysaccharides from seaweeds. *Carb Res,* **453-454**, 2017, 1-9.
14.XIONG, X., WANG, P., SUD, K., CHO, W.C., XING, Y., Chinese herbal medicine for coronavirus disease 2019: A systematic review and meta-analysis. *Pharm Res,* **160**, 2020, 105056.
15.O'BOYLE, N., BANCK, M., JAMES, C.A., MORLEY, C., VANDERMEERSCH, T., HUTCHISON, G.R., Open Babel: An open chemical toolbox. *J Chemoinform,* 2011.
doi: 10.1186/1758-2946-3-33.
16. SEELIGER, D., de GROOT, B.L., Ligand docking and binding site analysis with PyMOL and Autodock/Vina. *J Comput Aided Mol,* **24,** 2010, 417-422. doi 10.1007/s10822-010-9352-6.
17.AFIFAH, S., AMALIA, A., MASLIKAH, S.I., In silico study on flavonoids from red betel as microsomal Prostaglandin E Synthase-1 (mPGES-1) inhibitors in rheumatoid arthritis. *AIP Conf Proc,* **2120**, 2019, 080002; https://doi.org/10.1063/1.5115740.
18.TROTT, O., OLSON, A.J., AutoDock Vina: improving the speed and accuracy of docking with a new scoring function, efficient optimization and multithreading. *J Comp Chem,* 2010.
doi: 10.1002/jcc.21334.
19.CHEN, J., JIANG, H., LI, F., HU, B., WANG, Y., WANG, M., WANG, J., CHENG, M., Computational insight into dengue virus NS2B-NS3 protease inhibition: A combined ligand- and structure-based approach. *Comp Bio Chem,* **77,** 2018, 261-271
20. FISCHER, A., SELLNER, M., NERANJAN, S., SMIEŠKO, M., LILL, M.A., Potential Inhibitors for Novel Coronavirus Protease Identified by Virtual Screening of 606 Million Compounds. *Int J Mol Sci,* 2020. doi: 10.3390/ijms21103626.
21.SHARP, K.A., HONIG, B., Electrostatic interactions in macromolecules: theory and applications. *Annu Rev Biophys Chem.* **19,** 1990, 301-322.

Manuscript received: 10.07.2020